Acta Crystallographica Section B
Structural Science
ISSN 0108-7681

X-ray diffraction and packing analysis on vintage crystals: Wilhelm Koerner's nitrobenzene derivatives from the School of Agricultural Sciences in Milano

Francesco Demartin,[a] Giuseppe Filippini,[b]* Angelo Gavezzotti[a] and Silvia Rizzato[a]

[a]Dipartimento di Chimica Strutturale e Stereochimica Inorganica, Università di Milano, via Venezian 21, I-20133 Milano, Italy, and [b]Istituto di Scienze e Tecnologie Molecolari, CNR, c/o Dipartimento di Chimica Fisica, Università di Milano, via Golgi 19, I-20133 Milano, Italy

Correspondence e-mail: giuseppe.filippini@istm.cnr.it

Received 6 April 2004
Accepted 14 June 2004

The crystal structures of six nitrotoluene derivatives, synthesized by Wilhelm Koerner about a century ago and retrieved from a depository at the University of Milano, were determined. The correct assignment of molecular structures is verified. The geometry of the nitro groups and factors affecting the orientation of nitro groups with respect to the benzene ring are discussed, also using an auxiliary set of crystal structures retrieved from the Cambridge Structural Database. The crystal packings have been analyzed, and lattice energies have been calculated by atom–atom potential methods and by the newly proposed Pixel method. This method allows a more complete description of intermolecular potentials in terms of the interaction between molecular electron densities and separate Coulombic, polarization, dispersion and overlap repulsion energies. Lattice vibrations and external entropies were calculated by lattice-dynamical procedures. The results of the Pixel energy calculations allow a reliable, quantitative assessment of the relative importance of stacking interactions and hydrogen bonding in the rationalization of the recognition modes of nitrobenzene derivatives, which is impossible to attain using only qualitative atom–atom geometry concepts.

1. Introduction

Wilhelm Koerner (Kassel 1839–Milano 1925) began his career as an assistant to August Kekulé and Stanislao Cannizzaro. He worked in Milano in the first decades of the last century, at the Scuola Superiore di Agricoltura, where he specialized in the chemistry of halogen and nitrobenzene derivatives, carrying out the synthesis of a very large number of them. His results were instrumental in establishing the chemical proof of the equivalence of the six atoms in benzene, according to Kekulé's hypothesis, a story vividly summarized and chemically supplemented in a paper by McBride (1980), to which the reader is addressed for more chemical detail. Koerner was known to be almost a maniac for crystallization, although he was no crystallographer; careful analyses of many of his crystals were carried out by the famous Italian crystallographer Ettore Artini (see, for example, Artini, 1905, 1918). Artini's papers contain a description of morphology and polymorphism, frequent in these compounds, and the determination of the crystal system and of cell parameters by goniometric measurements. Interestingly, in those days the study of organic crystals was almost considered a perversion of crystallography; in the last paper of his series, Artini (1918) corrects some previous determinations ('*so grossly wrong as to constitute a reason for stupefaction*') and vindicates his work by saying: '*I would like this example to serve those who think that the crystallographic study of artificial substances is a sort of*

materia vile *to be left to beginners*'. He would have been happy to learn that nowadays the crystallography of organic compounds overwhelmingly outnumbers that of minerals, if only because of the relative abundance of samples.

A survey of the remnants of Koerner's collection of crystalline samples was carried out by one of us (A.G.) around 1990, by kind permission of the organic chemists of the School of Agriculture at the University of Milano. According to local witnesses, the site had unfortunately already been visited several times and the most impressive crystalline samples had been appropriated by unknown or forgotten collectors (although we were able to see an agglomerate, approximately 0.5 m high, of crystals of a sulfate salt, each of which was *ca* 5 cm across; we were told that sulfate salts were prepared only to add cohesion and mass to the crystallization products in order to produce impressive samples). More important for chemical crystallography was the finding of dozens of well preserved old-fashioned vials (see some examples in Fig. 1), each covered by a black cardboard cover, tightly sealed and labeled in elegant handwriting with the name of the compound (alas, no date). Each vial contained 1–10 g of crystals, mostly bright yellow, orange or red, with different morphologies, and appearing very well preserved after more than 80 years. From the general appearance of the samples and reports of the witnesses, we have reasons to believe that the vials were still in their original state and had not been altered or re-opened.

Table 1 summarizes the compounds and the crystal samples retrieved. Some of the samples were sent to Oxford where single-crystal X-ray diffraction analyses were carried out (Watkin, 2003); one of them has become a candidate in the 2004 Cambridge crystal structure prediction blind test (Day & Motherwell, 2003). The crystals of some other compounds had already been characterized and their crystal structures were retrieved from the Cambridge Database (Allen, 2002). We have undertaken an X-ray study of six of the remaining crystals as a historic final confirmation, if need be, of Koerner's assignments of molecular structures, which he of course had been made without the aid of spectroscopic or diffraction methods. The packing analysis of these crystals by modern molecular modeling tools (Gavezzotti, 2003*a*) further reveals the crystal chemistry of the aromatic nitro group and of the amide linkage.

Figure 1
Some of the original vials from the Koerner laboratory.

Table 1
The compounds retrieved.

CSD indicates that the crystal structure was already present in the Cambridge Structural Database. Acetammino or acetanilide: $-N(H)C(=O)CH_3$ group.

Original label on the vial (in italian)	Crystal structure symbol and space group (or CSD refcode)
2,6-Dinitro-3-acetamminotoluene	K6, $P2_1/c$, $Z = 4$
1,2,5-Nitroacetamminotoluene (= CSD MNIAAN10)	K12, $P2_1/c$, $Z = 4$
1,3-Bromoiodo-6-nitro-4-acetanilide	K15, $P\bar{1}$, $Z = 2$
3,4,5-Trinitrotoluene	K19 $C2/c$, $Z = 4$
2,3,4-Trinitrotoluene (forma β)	K20, $P\bar{1}$, $Z = 2$
1,6-Dinitro-2,4-toluidina (2,6-dinitro-1,4-toluidine)	K14, $Cmc2_1$ two half molecules in the asymmetric unit
2,6-Dinitro-3,5-dibromotoluene	K5 (disordered)
1-Nitro-3,5-dimetossi-4-anilina	Not determined
3,6-Dinitro-2-amminotoluene	Not determined
3,5-Dinitro-2-chlorotoluene	Not determined
3,5-Dinitro-4-bromotoluene	Not determined
2-Nitro-4-bromotoluene	Not determined
2,6-Dinitro-3-iodotoluene	Determined in Oxford
3,6-Dinitro-2-acetamminotoluene	Determined in Oxford
4-Nitro-2-acetamminotoluene	Determined in Oxford
4,5-Dinitro-2-acetamminotoluene	Determined in Oxford
2,4-Dinitrotoluene	CSD, ZZZGVU01
5-Nitro-2-amminotoluene	CSD, BAJCIY01
3-Nitro-4-acetamminotoluene	CSD, MNIAAN01, MNIAAN02, MNIAAN10

2. Experimental

The vials were opened with great care, but without special precautions or difficulties. Only gentle tapping or warming of the glass stopcocks was sometimes necessary. The materials appeared in an excellent state of preservation, thanks to the thick black cardboard covers that prevented exposure to light, and to the fact that the vials were sealed airtight. For security reasons, large amounts of potentially dangerous nitro derivatives had to be disposed of by dissolution, and only *ca* 1 g of each substance was retained. A list of the compounds with preliminary information is given in Table 1. Three polymorphic crystal structures of compound K12 had been determined previously, but it was decided to carry out a crystal structure determination on our material, to check the stability of the particular polymorphic form. All the X-ray crystal structure determinations used single crystals picked directly from the original batch samples and cut to suitable dimensions. No recrystallization was necessary.

2.1. Crystallography

The data collections were performed at room temperature on a SMART-CCD Bruker diffractometer, by the ω-scan method. Empirical absorption corrections were applied (*SADABS*; Sheldrick, 1996) in all cases. The structure was

Table 2
Experimental data.

	K15	K19	K20
Crystal data			
Chemical formula	$C_8H_6BrIN_2O_3$	$C_7H_5N_3O_6$	$C_7H_5N_3O_6$
M_r	384.96	227.14	227.14
Cell setting, space group	Triclinic, $P\bar{1}$	Monoclinic, $C2/c$	Triclinic, $P\bar{1}$
a, b, c (Å)	4.797 (2), 7.673 (2), 15.654 (4)	13.6440 (10), 9.550 (1), 8.754 (1)	7.700 (2), 8.329 (2), 8.694 (2)
α, β, γ (°)	96.98 (2), 97.03 (2), 103.34 (2)	90, 121.31 (2), 90	87.890 (10), 65.100 (10), 67.330 (10)
V (Å^3)	549.7 (3)	974.53 (17)	461.40 (19)
Z	2	4	2
D_x (Mg m^{-3})	2.326	1.548	1.635
Radiation type	Mo $K\alpha$	Mo $K\alpha$	Mo $K\alpha$
No. of reflections for cell parameters	3296	837	855
θ range (°)	2–25	2–22	2–22
μ (mm^{-1})	6.54	0.14	0.15
Temperature (K)	293 (2)	293 (2)	293 (2)
Crystal form, color	Column, yellow	Block, very light yellow	Column, light yellow
Crystal size (mm)	0.3 × 0.25 × 0.15	0.36 × 0.3 × 0.26	0.4 × 0.2 × 0.2
Data collection			
Diffractometer	SMART	SMART	SMART
Data collection method	ω scan	ω scan	ω scan
Absorption correction	*SADABS*	*SADABS*	*SADABS*
T_{min}	0.62	0.79	0.94
T_{max}	1	1	1
No. of measured, independent and observed reflections	4680, 1947, 1799	2636, 763, 585	3177, 1165, 1023
Criterion for observed reflections	$I > 2\sigma(I)$	$I > 2\sigma(I)$	$I > 2\sigma(I)$
R_{int}	0.034	0.032	0.024
θ_{max} (°)	25	24	23
Range of h, k, l	$-5 \Rightarrow h \Rightarrow 5$ $-9 \Rightarrow k \Rightarrow 9$ $-18 \Rightarrow l \Rightarrow 18$	$-15 \Rightarrow h \Rightarrow 13$ $-10 \Rightarrow k \Rightarrow 10$ $-8 \Rightarrow l \Rightarrow 9$	$-8 \Rightarrow h \Rightarrow 8$ $-8 \Rightarrow k \Rightarrow 8$ $-9 \Rightarrow l \Rightarrow 9$
Refinement			
Refinement on	F^2	F^2	F^2
$R[F^2 > 2\sigma(F^2)]$, $wR(F^2)$, S	0.031, 0.098, 1.09	0.034, 0.147, 0.81	0.037, 0.111, 1.06
No. of reflections	1947	763	1165
No. of parameters	136	75	145
H-atom treatment	Mixture of independent and constrained refinement	Mixture of independent and constrained refinement	Mixture of independent and constrained refinement
Weighting scheme	$w = 1/[\sigma^2(F_o^2) + (0.068P)^2]$, where $P = (F_o^2 + 2F_c^2)/3$	$w = 1/[\sigma^2(F_o^2) + (0.1341P)^2 + 0.2249P]$, where $P = (F_o^2 + 2F_c^2)/3$	$w = 1/[\sigma^2(F_o^2) + (0.059P)^2 + 0.1766P]$, where $P = (F_o^2 + 2F_c^2)/3$
$(\Delta/\sigma)_{max}$	0.013	0.004	0.017
$\Delta\rho_{max}$, $\Delta\rho_{min}$ (e Å^{-3})	0.59, −1.48	0.15, −0.15	0.24, −0.21

	K6	K12	K14
Crystal data			
Chemical formula	$C_9H_9N_3O_5$	$C_9H_{10}N_2O_3$	$C_{14}H_{14}N_6O_8$
M_r	239.19	194.19	394.31
Cell setting, space group	Monoclinic, $P2_1/c$	Monoclinic, $P2_1/c$	Orthorhombic, $Cmc2_1$
a, b, c (Å)	9.686 (2), 11.368 (2), 9.976 (2)	10.430 (2), 9.991 (2), 9.574 (2)	12.239 (2), 10.582 (2), 13.582 (3)
β (°)	98.74 (2)	99.510 (10)	90
V (Å^3)	1085.7 (4)	984.0 (3)	1759.0 (6)
Z	4	4	4
D_x (Mg m^{-3})	1.463	1.311	1.489
Radiation type	Mo $K\alpha$	Mo $K\alpha$	Mo $K\alpha$
No. of reflections for cell parameters	1024	912	790
θ range (°)	2–25	2–23	2–24
μ (mm^{-1})	0.12	0.1	0.12
Temperature (K)	293 (2)	293 (2)	293 (2)
Crystal form, color	Column, bright yellow	Needle, light yellow	Orange, needle
Crystal size (mm)	0.4 × 0.26 × 0.26	0.4 × 0.12 × 0.12	0.32 × 0.14 × 0.12
Data collection			
Diffractometer	SMART	SMART	SMART
Data collection method	ω scan	ω scan	ω scan
Absorption correction	*SADABS*	*SADABS*	*SADABS*

Table 2 (continued)

	K6	K12	K14
T_{min}	0.79	0.92	0.89
T_{max}	1	1	1
No. of measured, independent and observed reflections	8680, 1917, 1610	8196, 1735, 1147	4779, 1416, 1243
Criterion for observed reflections	$I > 2\sigma(I)$	$I > 2\sigma(I)$	$I > 2\sigma(I)$
R_{int}	0.027	0.039	0.026
θ_{max} (°)	25	25	25
Range of h, k, l	$-11 \Rightarrow h \Rightarrow 11$ $-13 \Rightarrow k \Rightarrow 13$ $-11 \Rightarrow l \Rightarrow 11$	$-12 \Rightarrow h \Rightarrow 12$ $-11 \Rightarrow k \Rightarrow 11$ $-11 \Rightarrow l \Rightarrow 11$	$-14 \Rightarrow h \Rightarrow 14$ $-12 \Rightarrow k \Rightarrow 8$ $-15 \Rightarrow l \Rightarrow 15$
Refinement			
Refinement on	F^2	F^2	F^2
$R[F^2 > 2\sigma(F^2)]$, $wR(F^2)$, S	0.051, 0.165, 1.06	0.048, 0.157, 1.04	0.037, 0.119, 1.15
No. of reflections	1917	1735	765
No. of parameters	154	127	140
H-atom treatment	Mixture of independent and constrained refinement	Mixture of independent and constrained refinement	Mixture of independent and constrained refinement
Weighting scheme	$w = 1/[\sigma^2(F_o^2) + (0.092P)^2 + 0.5057P]$, where $P = (F_o^2 + 2F_c^2)/3$	$w = 1/[\sigma^2(F_o^2) + (0.0705P)^2 + 0.4277P]$, where $P = (F_o^2 + 2F_c^2)/3$	$w = 1/[\sigma^2(F_o^2) + (0.0757P)^2 + 0.3587P]$, where $P = (F_o^2 + 2F_c^2)/3$
$(\Delta/\sigma)_{max}$	0.001	<0.0001	0.717
$\Delta\rho_{max}$, $\Delta\rho_{min}$ (e Å^{-3})	0.30, −0.27	0.23, −0.21	0.19, −0.17

Computer programs: *SIR2000* (Burla *et al.*, 2001), *SHELXL97* (Sheldrick, 1997), *SCHAKAL99* (Keller, 1999).

solved by direct methods (*SIR*2000; Burla *et al.*, 2001) and refined by full-matrix least-squares on F^2 (*SHELXL*97; Sheldrick, 1997) with a *WINGX* interface (Farrugia, 1999). Anisotropic displacement parameters were assigned to all non-H atoms, while H atoms were put in calculated positions and refined using a riding model. Crystallographic data and analysis parameters are given in Table 2. Tables S1 and S2 (deposited) contain bond lengths and bond angles.[1]

4-Methyl-2-nitroacetanilide (or 3-nitro-4-acetamidotoluene) is remarkable in that it packs in three polymorphs, two of which (CSD refcodes MNIAAN01 and MNIAAN02) form intramolecular N—H···O═N hydrogen bonds (Moore *et al.*, 1983). Our determination of the crystal structure of the Koerner material reveals that we have MNIAAN10 and confirms the structure of the monoclinic white polymorph. Our finding of an apparently pure crystal form after so many years reveals that either this is the most stable polymorph or that no easy phase transformation may occur in this system.

The determination of the crystal structure of compound K5 was also carried out. The structure is disordered as a result of the partial population of a molecular position rotated by approximately 60° so that substituents of approximately the same size and diffracting power overlap, except at the hydrogen position which is partly occupied by bromine, resulting in a spurious electron-density peak. The chemical composition was thus confirmed, but no further molecular structure or crystal packing analyses were carried out. Details of this crystal structure are available from the authors upon request.

[1] Supplementary data for this paper are available from the IUCr electronic archives (Reference: NA5014). Services for accessing these data are described at the back of the journal. See www.rsc.org/suppdata/ for crystallographic files in cif format.

3. Computational and simulation methods

All the compounds and crystal structures determined were analyzed for structural effects on molecular conformation and crystal packing. A group of related compounds (Table 3) were retrieved from the Cambridge Structural Database for assistance and comparisons in the analysis, which uses comprehensive descriptors and intermolecular potential energy calculations. We consider some molecular fragments comprising nearly planar atom groups: rings, defined by the six atoms in a benzene ring; nitro groups, defined by the N and O atoms plus the C atom to which they are attached; acetamido groups, defined by the atoms of the C(CO)N linkage. Angles between pairs of these groups were then calculated as the angle (normalized to the 0–90° range) between the vectors perpendicular to the group planes. Short atom–atom intermolecular distances were recognized and classified, especially O···H distances over the amide hydrogen bonds. We also use the concept of a structure determinant (Gavezzotti & Filippini, 1995): picking a reference molecule in a crystal structure (the choice is arbitrary), each structure determinant is a molecular pair formed by the reference and a surrounding molecule, characterized by a distance between centers of mass, a symmetry operator connecting the two molecules and a molecule–molecule energy. Molecular pairs at short distances usually have the highest interaction energies. The collection of all molecules which have a significant interaction energy with the reference molecule constitutes the coordination sphere; their number is usually around 12, the number of nearest-neighbors in a close-packed arrangements of spheres.

For a quantitative discussion of packing effects, intermolecular energies are needed. For a simple and quick approach, they were computed by the UNI atom–atom potentials of Gavezzotti & Filippini (1994), sometimes

Table 3
Crystal structures of related compounds retrieved from the Cambridge Structural Database.

	Refcode	Notes
1,2-Dinitrobenzene	ZZZFYW01	$P2_1/c$, $Z = 4$
1,3-Dinitrobenzene	DNBENZ10	$Pbn2_1$, $Z = 4$
1,4-Dinitrobenzene	DNITBZ11	$P2_1/n$, $Z = 2$
4-Nitrotoluene	NITOLU	$Pcab$, $Z = 8$
1,3,5-Trinitrobenzene	TNBENZ10	$Pbca$, $Z = 16$
1,3,5-Trinitrotoluene	ZZZMUC01	$Pca2_1$, $Z = 8$
	ZZZMUC06	$P2_1/b$, $Z = 8$
2,6-Dinitrotoluene	ZZZQSC	$P2_12_12_1$, $Z = 4$
2,6-Dinitro-3-chlorotoluene	BAFLEZ	$P\overline{1}$, $Z = 2$
1,4-Dimethyl-2-chloro-3,5-dinitrobenzene	CMNBEN10	$Pna2_1$, $Z = 4$

supplemented by atom–atom point-charge Coulombic terms over atomic charge parameters obtained from the ESP procedure embedded in the *GAUSSIAN* program (Frisch *et al.*, 1998). Experience on nitro compounds had already been gained (Filippini & Gavezzotti, 1994). A more reliable evaluation of intermolecular interactions is obtained by the Pixel method (Gavezzotti, 2002, 2003*b*). In this approach the molecular electron density is first calculated by standard quantum chemical methods, giving a delocalized description of the electron distribution by a large number (*ca* 10 000) of negatively charged pixels. The Coulombic energy is then calculated by sums over pixel–pixel, pixel–nucleus and nucleus–nucleus Coulombic terms. A local polarizability is then assigned to each pixel. The electric field generated by pixels and nuclei in surrounding molecules is calculated and the polarization energy is evaluated; an empirical damping function is introduced to avoid singularities. A London-type formula is used to evaluate dispersion energies, through the local pixel polarizabilities and the molecular ionization potential, taken as the energy of the highest occupied molecular orbital. This last calculation requires another damping function with a second empirical parameter. Finally, the overlap between molecular densities is calculated and the exchange repulsion energy is evaluated as being proportional to the overlap integral raised to a power between 0.9 and 1.0. The proportionality constant and the exponent are two more parameters. The numerical values of the four parameters were derived as described in detail elsewhere (Gavezzotti, 2003*c*).

The Pixel method has been applied successfully to the calculation of energies of gas-phase dimers, where it has been demonstrated (Gavezzotti, 2003*c*) that the quality of the Pixel results is often similar to that of quantum chemical calculations, at a fraction of the computational cost. What is more important here is that the Pixel method allows the calculation of lattice energies in good agreement with crystal sublimation enthalpies for a wide selection of organic compounds, and also performs well in the energy ranking for polymorphs of organic crystal structures (Gavezzotti, 2003*d*).

Quantum mechanical molecular energies and electron densities, as well as ESP atomic point-charge parameters, were calculated by *Gaussian* (Frisch *et al.*, 1998) at the MP2/6-31G** level. All molecular geometries were fixed as extracted from the corresponding crystal structures. The lattice energies were calculated by including in the crystal model all molecules up to a separation between molecular centers of 18 Å. All crystal-packing analysis calculations were carried out using the *OPiX* program package (Gavezzotti, 2003*a*), which includes a packing analysis and lattice energy calculation module (Zip-Opec module), a polymorph-generation module, including a lattice energy minimizer (Zip-Promet-Minop module) and a module for the calculation of the dimer and lattice energies by the Pixel method (Pixel module).

In an attempt to describe the internal dynamics of these crystals, which cannot be taken into account by the static potential energy methods so far described, calculations of lattice vibration frequencies and of external contributions to crystal entropies and specific heats were performed by a lattice dynamical procedure in the rigid-molecule approximation (Gramaccioli & Filippini, 1984), also using the UNI empirical atom–atom potentials.

Table 4
Dihedral angle between the phenyl ring and the nitro groups, as a function of the two adjacent substituents on the ring, for the complete sample of the 22 crystal structures considered.

Substituents	Range (°)	No. of observations
H, H	0–33	16
CH_3, H	29–60	17
CH_3, Cl	80–86	2
Br, H	28	1
NO_2, H	27–41	4
CH_3, NO_2	59	1
NO_2, NO_2	64–67	2

3.1. Intramolecular geometry and conformation

Typical s.u.'s on bond distances are 0.002–0.007 Å and on angles 0.2–0.4°. The 26 N—O bond distances in the 13 crystallographically different nitro groups span the range 1.202–1.225 Å, with an average of 1.215 Å. The 13 corresponding O—N—O bond angles span the range 122.8–125.8°, with an average of 124.3°. The C—N(nitro) bond distance spans the range 1.462–1.484 Å, with an average of 1.472 Å. In all cases, deviations from the average value are mostly within three times the s.u. All other bond distance and angle parameters are within the expected ranges.

The angle between the plane of the phenyl rings and that of the nitro groups spans an almost complete 0–90° range. There seems to be a moderate correlation (Table 4) between the phenyl–nitro dihedral angle and the bulk and/or the polarity of the adjacent groups: the angle is smallest for two H atoms, increases for one hydrogen and a methyl group, and is very large for a methyl group and a Cl atom or for two nitro groups. Otherwise, the phenyl–nitro dihedral angle seems to be rather prone to deformation by packing forces, because it can easily vary by *ca* 30° for the same adjacent substituents.

An estimate of the shape of the potential energy barrier for nitro-group rotation was obtained by an MP2/6-31G** calculation on nitrobenzene, using a fixed geometry for the molecule as obtained from an average of the molecular dimensions in the nitrobenzenes in our sample (ring C—C 1.38 Å, all ring

Table 5
Relative energies and charges in isomeric aromatic nitro derivatives.

MP2/6-31G** calculation; energies in kJ mol^{-1}; ESP charges in electrons.

	Relative energy	Charge on nitro N	Charge on nitro O	Phenyl–nitro angles (°)
1,2-Dinitrobenzene	+28.0	0.633	−0.335 to −0.361	41, 41
1,3-Dinitrobenzene	+14.1	0.614, 0.580	−0.350 to −0.367	11, 15
1,4-Dinitrobenzene	0	0.638	−0.369	10, 10
3,4,5-Trinitrotoluene	+20.5	0.640	−0.316 to −0.364	32, 67, 32
2,3,4-Trinitrotoluene	+22.0	0.632 to 0.691	−0.330 to −0.359	59, 64, 27
2,4,6-Trinitrotoluene	0	0.624 to 0.695	−0.356 to −0.372	40, 33, 60

angles 120°, C—N 1.48 Å, N═O 1.22 Å, O═N═O angle 125°) and varying the dihedral angle between the plane of the ring and the plane of the nitro group. The result (Fig. 2) shows a preference for the planar conformation over the perpendicular one by 24 kJ mol^{-1}, but also a deformation of 30° for an energy loss equal to the room-temperature value of RT, in line with the observed flexibility upon the action of intramolecular steric requirements and of packing forces. At the same time, the charge separation over the nitro group increases from q_N = +0.590, q_O = −0.363 at the planar conformation to q_N = +0.693, q_O = −0.390 at the perpendicular conformation, so that point charges are sensitive to the twist angle between the nitro group and the benzene ring. These results demonstrate that any attempt at the prediction of the crystal structure of nitro compounds must take into account nitro group rotation, a very problematic task.

Table 5 shows the relative molecular energies of some isomers, calculated at the MP2/6-31G** level with molecular geometries as found in the crystal. For the dinitrobenzenes, the trend seems to follow from some electronic effect due to the position of the substituents, or to steric effects due to the proximity of the nitro groups, rather than from the non-coplanarity of the nitro groups and the phenyl ring; in fact, the energy cost of rotation up to 40° does not exceed 5 kJ mol^{-1} (see Fig. 2) and cannot explain the large difference between the 1,2- and the 1,4-isomers. For the trinitrotoluene isomers, phenyl–nitro dihedral angles are more or less equivalent; the more symmetrical and less overcrowded isomers are more stable.

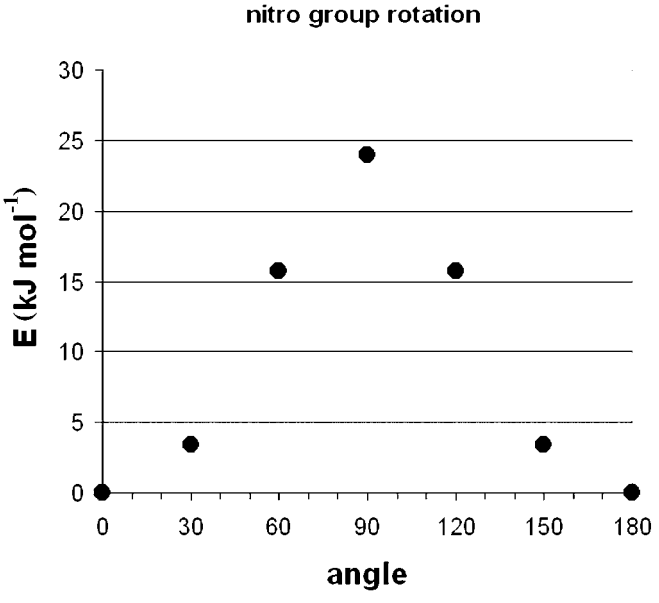

Figure 2
Quantum chemical result for the potential energy barrier for the rotation of the nitro group plane with respect to the phenyl ring plane in nitrobenzene.

4. Packing analysis

As already mentioned, we use a breakdown of lattice interaction energies into molecule–molecule terms between nearest neighbors, which we call structure determinants. Table 6 collects these structural determinants for the crystals studied here. The Pixel calculation is not feasible for K14, because there are two molecules in the asymmetric unit, or for K15, because of the iodine and bromine substituents.

4.1. K6, 2,6-dinitro-3-acetamidotoluene

The planes of the two nitro groups form a large angle with the plane of the phenyl ring (52 and 53°) and there is no intramolecular interaction between the neighboring nitro and acetamido groups; the plane of the acetamido group is also twisted at a high angle (50°) with respect to the phenyl ring. There is a N—H···O═C hydrogen-bonding chain (H···O distance 1.94 Å) riding a glide plane running along c, which can be seen in the motif shown in Fig. 3. However, the dominating structural determinant is a stacking interaction (Fig. 4) between molecules related by a center of symmetry. This determinant gains stabilization mainly from dispersion contributions, although the electrostatic contribution is also substantial. The hydrogen-bonding determinant ranks second in energy and gains mostly from the electrostatic component, as expected. Hydrogen-bonding energies may well vary by 5–10 kJ mol^{-1} for very small variations of the hydrogen-bonding distance, and we do not put too much trust on the absolute value for this energy. Nevertheless, on the basis of these results, one can say that hydrogen bonding is not the sole, and not even the main, driving force for the crystallization of this compound.

4.2. K14, 2,6-dinitro-4-aminotoluene

Each of the two molecules in the asymmetric unit lies on a mirror plane, so that all the benzene ring planes are parallel in the crystal. There are several N—H···O═N short atom–atom contacts (2.24 and 2.42 Å) which could be called weak hydrogen bonds, over a centering operation. Judging from

Table 6
The structure determinants.

A determinant is a pair of close-neighbor molecules in the crystal. For each determinant: symbol of the symmetry operator (I inversion center, G glide plane, S screw axis, T translation, AU two molecules in the asymmetric unit), distance between molecular centers of mass, interaction energy by the atom–atom UNI force field, Pixel Coulombic, polarization, dispersion, repulsion and total interaction energies (kJ mol^{-1})

E_{UNI}	E_{coul}	E_{pol}	$E_{energy\text{-}dispersive}$	E_{rep}	E_{tot}
K6, I1, 4.75, −54.7	−25.8	−3.3	−42.6	20.8	−50.9
G1, 7.82, −32.4	−40.4	−8.3	−18.2	43.6	−23.3
I2, 5.13, −32.8	−10.6	−2.3	−26.1	18.5	−20.5
G2, 7.32, −18.9	−5.2	−1.0	−14.2	10.4	−10.0
K14, AU, 4.48 −46.8	–	–	–	–	–
AU+S, 4.33, −44.0	–	–	–	–	–
C, 8.09, −15.6	–	–	–	–	–
K15, Tx, 4.80, −61.7	–	–	–	–	–
I, 9.68, −14.8	–	–	–	–	–
I, 9.67, −14.9	–	–	–	–	–
K19, G1, 4.55, −38.7	−27.8	−3.3	−38.4	22.2	−47.3
G2, 6.86, −21.6	−12.6	−1.6	−19.2	10.0	−23.4
C, 8.33, −11.7	−5.4	−1.4	−9.6	7.4	−9.0
K20, I1, 4.05, −55.6	−24.2	−3.2	−52.0	23.6	−55.8
I2, 4.34, −39.5	−28.8	−3.6	−41.4	27.6	−46.2
I3, 7.09, −17.8	−3.0	−1.1	−16.2	2.8	−17.5
$T(x)$, 7.70, −13.2	−10.6	−1.4	−12.0	10.6	−13.4
NITOLU, I, 3.52, −40.0	−12.6	−1.4	−40.0	16.4	−37.6
G, 4.86, −20.0	+0.2	−1.3	−22.8	10.2	−13.7

UNI atom–atom energies, the main source of cohesion, however, originates from the stacking interactions between two antiparallel molecules in the asymmetric unit (one of these stacked dimers is shown in Fig. 5). Fig. 6 shows the impressive layered packing of this compound.

4.3. K15, 2-nitro-4-acetamido-5-iodo-bromobenzene

There is an N—H···O=C hydrogen bond chain formed by translation along *a* (Fig. 7, H . . . O 1.948 Å), which is by far the most stabilizing structural determinant, as it generates both the hydrogen bond and a stacking of the benzene ring planes. The other apparently relevant packing motif is a layered structure (Fig. 8) with short Br···O (3.212 Å) and I···O (3.071 Å) atom–atom contacts. The frequency of appearance of such short intermolecular atom–atom distances has been analyzed (Lommerse *et al.*, 1996).

4.4. K19, 3,4,5-trinitrotoluene and K20, 2,3,4-trinitrotoluene $P\bar{1}$, Z = 2

In the crystal of the 3,4,5-isomer the molecule retains a twofold symmetry axis, which implies disorder in the methyl-group hydrogen positions. The most stabilizing structure determinant (47.3 kJ mol^{-1} of cohesive energy, Table 6) is a stacking interaction generated by a glide plane along the *c* direction, where intuitive rules based on overall molecular dipoles are patently violated (Fig. 9) because molecular ends containing the nitro groups are close to one another; and yet this determinant has a substantial stabilizing Coulombic energy. The second best determinant is another stacked antiparallel dimer. In fact, molecules are all parallel in this crystal and pack in a checkerboard layer pattern in the *ab* plane, because of the centering operation (Fig. 10), in which positively charged methyl and aromatic hydrogen regions are opposed to nitro groups. These could be called C—H···O hydrogen bonds, but their influence is only marginally stabi-

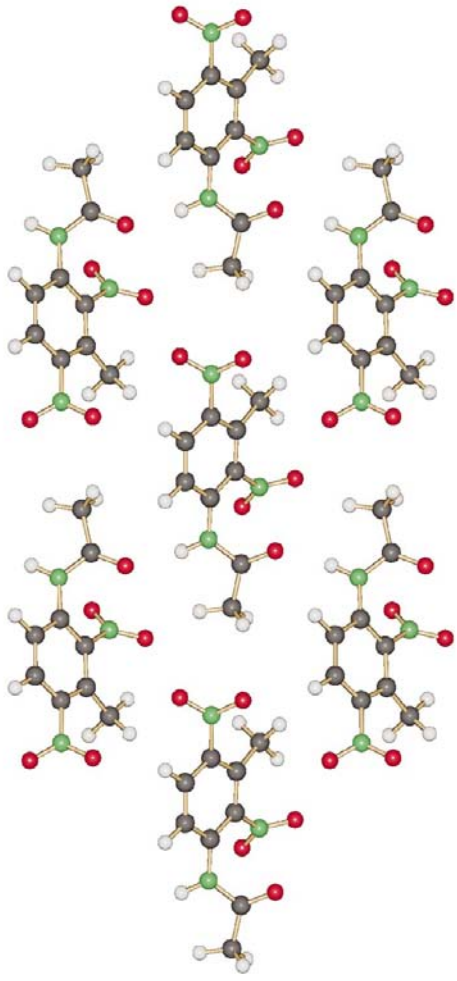

Figure 3
A layer in the *bc* plane of the crystal structure of compound K6. The hydrogen-bonding chain (O···H 1.94 Å, O···H—N angle 163°) running along *c* (horizontal) can be seen, corresponding to determinant G1 in Table 6.

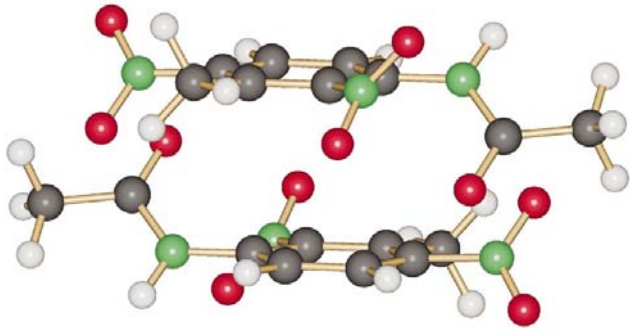

Figure 4
The energetically most relevant pair interaction (structure determinant I1, see Table 6) in the crystal structure of K6. Symmetry code: $1-x, -y, -z$.

lizing (see the centering structure determinant for K19 in Table 6, with only 9 kJ mol^{-1} of cohesive energy).

The main structure determinants in the crystal of the 2,3,4-isomer, K20, are again contacts between inversion-related, and hence antiparallel, stacked aromatic ring planes (Fig. 11), with substantial stabilizing Coulombic and dispersion energy contributions. Translational propagation perpendicular to these stacking interactions forms molecular layers in the *ac* plane (Fig. 12), in which the recognition problem is solved by opposing the negatively charged molecular moiety carrying the nitro groups to the positively charged aromatic hydrogen rim. There is one short O$\cdots$H distance of 2.38 Å, and yet the Pixel calculation reveals that these structure determinants are far from ranking high in the energetic demands of the crystal packing of this compound (13.4 against 46–56 kJ mol^{-1} for the stacking determinants). These results reveal that short atom–atom distances do not always correspond to high-priority recognition modes and this casts some doubt on the

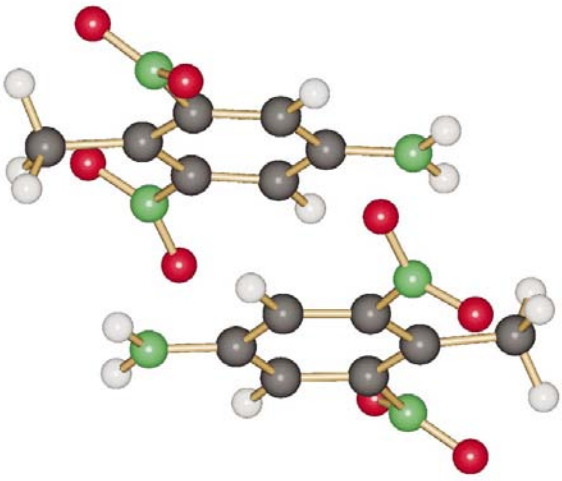

Figure 5
The main structure determinant, AU in Table 6, in the crystal structure of K14 (symmetry code $1-x, 1-y, \frac{1}{2}+z$). The angles between the planes of the nitro groups and the aromatic ring are 38 and 40°.

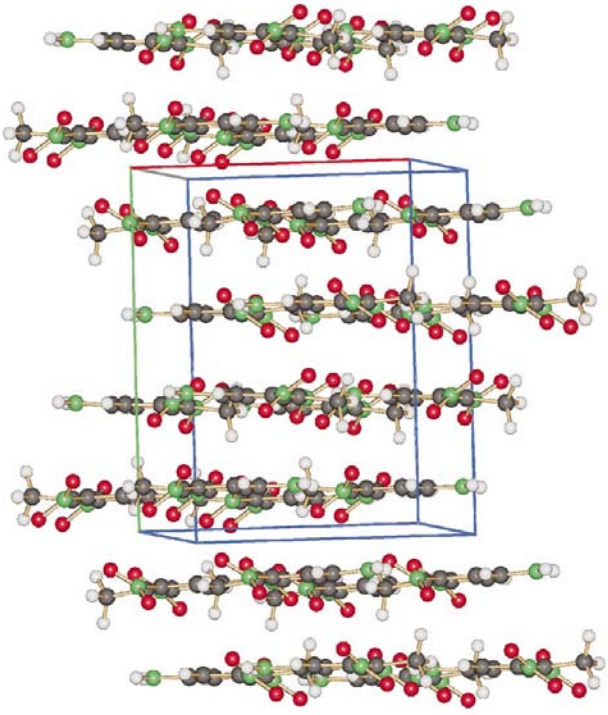

Figure 6
The layered crystal structure of compound K14.

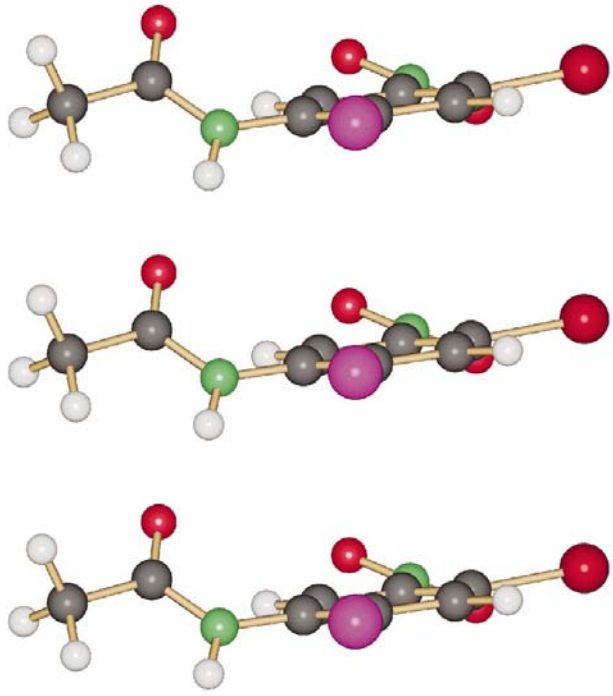

Figure 7
Translation along *a*, vertical in this figure, in the crystal structure of compound K15 [determinant $T(x)$, Table 6]. The vertical hydrogen-bonding chain is evident (O$\cdots$H 1.95 Å, O$\cdots$H—N angle 163°). The angle between the plane of the acetamido group and that of the benzene ring is 46°, the angle between the nitro group and the benzene ring is 28°.

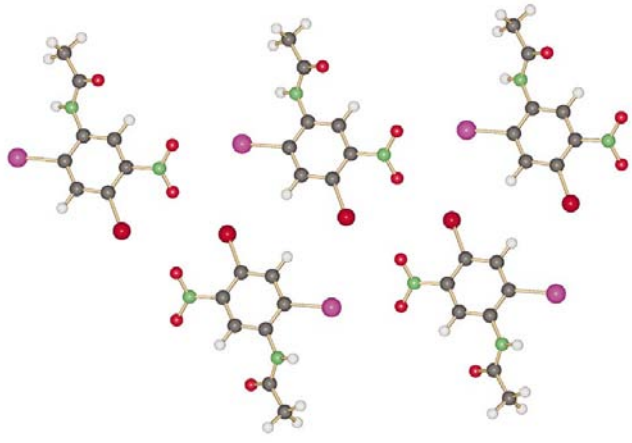

Figure 8
A layer in the crystal structure of compound K15 (symmetry codes $x-1, 1+y, z$; $1+x, y-1, z$; and the two I determinants in Table 6: $2-x, -y, 2-z$; $1-x, 1-y, 2-z$). The *a* axis is horizontal.

significance of C—H···O hydrogen bonds in the crystal chemistry of aromatic nitro compounds.

4.5. The arrangement of benzene rings

Fig. 13 plots the angles between all benzene rings in the crystals of the compounds considered here, as a function of the distance between ring centers. There is an obvious predominance of parallel or nearly parallel ($0 < \varphi < 15^\circ$) arrangements at a short distance, but when the distance between ring centers becomes large enough (> 6 Å) the angle between benzene rings spans the full 0–90° range. One outlier is a molecular pair in the 4-nitrotoluene crystal structure, with a very close ring–ring contact (distance of 4.78 Å) and a high angle, 46°. It would be tempting to take the picture of this pair (G determinant of Table 6 and Fig. 14) as evidence of crystal stabilization owing to some C—H···π interaction or 'hydrogen bond'. However, as Fig. 14 also shows, the main structure determinant in the 4-nitrotoluene crystal structure is the I determinant in Table 6, again an antiparallel stacked dimer at a very short (3.51 Å) interplanar distance, while the pair with the particularly short C···H distances is much less stabilizing and, in particular, the Coulombic energy in that pair is destabilizing. These results issue a warning against hasty energetic conclusions on the basis of molecular geometries alone.

The plot in Fig. 13 is also obviously biased by the ubiquitous presence of pure translation in crystals. The distance between benzene rings does not seem to correlate in any way with the angle between ring planes, outside the strict range of sharp steric repulsion.

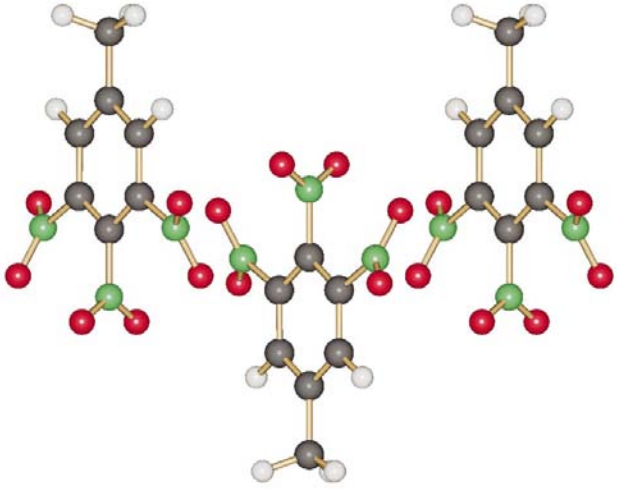

Figure 9
Stacking of molecular planes in the crystal structure of compound K19, corresponding to the most stabilizing structure determinant, G1, in Table 6 (symmetry codes: $x, 2-y, \frac{1}{2}+z$; $x, 2-y, z-\frac{1}{2}$; the c direction is horizontal). The nitro ends of the overall molecular dipole are close to one another.

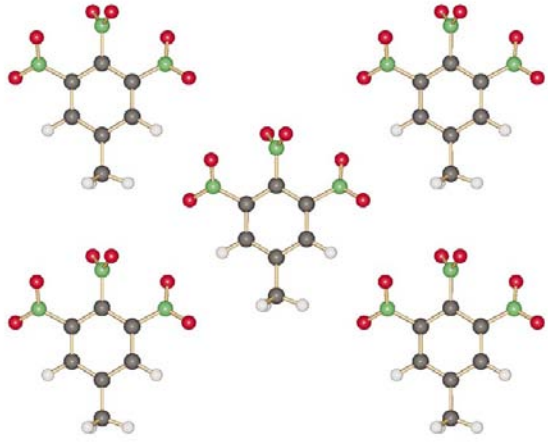

Figure 10
A layer in the crystal structure of compound K19 (C centering).

4.6. Short atom–atom contacts; further analysis

Packing analyses in organic crystals are often conducted on the basis of selected atom–atom intermolecular distances. Our previous and present experience does not encourage this practice, since there is nothing in the intermolecular field that depends on the mutual position of atomic nuclei alone, and inferences based only on short distances between atoms may be misleading. We prefer the analysis of recognition modes of molecular groups or of molecular zones of predictable polarity, although nothing can substitute for a quantitative analysis based on intermolecular energies. Nevertheless, in some cases short atom–atom distances reveal the existence of attractive interactions between molecular regions; we concentrate here on C—H groups at the rim of the benzene rings and on methyl groups, as potentially positively charged

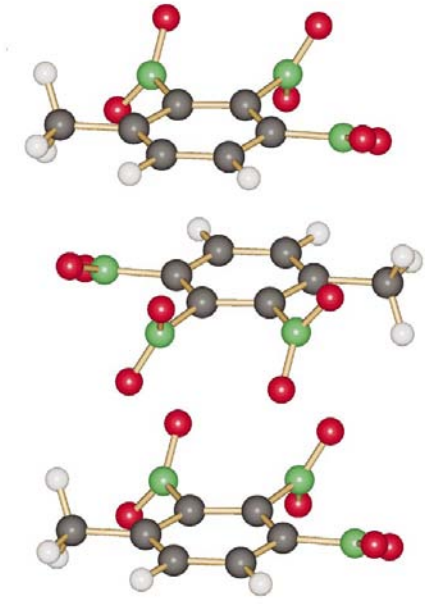

Figure 11
Tight stacking in the crystal structure of compound K20, corresponding to the two topmost structure determinants, I1 and I2 (symmetry codes: $1-x, -y, 1-z$; $1-x, 1-y, 1-z$).

Table 7
PIXEL lattice energies in the crystals of nitro compounds.

Pixel Coulombic, polarization, dispersion, repulsion and total lattice energies; lattice energies with the UNI atom–atom force field; sublimation enthalpy (kJ mol^{-1})

Compound	E_{coul}	E_{pol}	E_{disp}	E_{rep}	E_{tot}	E(UNI)	ΔH(subl)
1,2-Dinitrobenzene	−36.5	−9.1	−87.8	42.3	−91	−101	87.9
1,3-Dinitrobenzene	−30.7	−9.0	−91.0	45.2	−86	−101	87.0
1,4-Dinitrobenzene	−38.7	−10.6	−89.7	49.4	−90	−105	96.2
4-Nitrotoluene	−23.0	−7.0	−76.0	37.6	−68	−86	79.0
3,4,5-Trinitrotoluene	−48.2	−12.7	−93.9	54.3	−100	−112	113.3
2,3,4-Trinitrotoluene	−42.4	−12.1	−102.6	57.1	−100	−120	
1,3,5-Trinitrobenzene	–	–	–	–	–	−105	107.1

groups, against the zone of negative charge that surrounds the nitro O atoms.

The frequency of appearance of short distances between H atoms and nitro O atoms is shown in Fig. 15. Ring H atoms point towards nitro groups more frequently than methyl H atoms, but the difference is barely significant, partly because of the small number of structures available. In any case, our distribution here shows nothing different from the overall distribution of O···H distances (Rowland & Taylor, 1996) where the range between 2.2 and 2.6 Å is rather substantially populated. Besides, as shown above, the main structural determinants in the crystal packing of these molecules come from stacking interactions, which prevent, at least to some extent, C—H···O interactions. From our analysis, we do not see compelling evidence for considering these bonds as relevant in the determination of the main structural features of our crystals.

5. Accurate evaluation of lattice energies

Table 7 shows the calculated lattice energies. All three kinds of energies (Coulombic polarization, dispersion and repulsion) increase with molecular size. For all the compounds considered, the bulk of the lattice energy comes from dispersion. In fact, the total lattice energies almost coincide with the dispersion contributions, due to an almost exact cancellation of repulsion against the sum of electrostatic and polarization energies; this contradicts a common view, according to which the lattice energy of crystals of polar compounds should be the same as with the electrostatic contribution. Experience with these as well as with many other organic crystals shows, however, that the Coulombic energy takes on a dominant role as soon as hydrogen bonding is present. Lattice energy differences among isomers apparently depend on small differences in various contributions; for example, for the dinitrobenzenes the Coulombic energy favors the 1,4-isomer (notice how lattice Coulombic energies have no correlation with molecular dipoles), but the smaller density of the 1,2-isomer allows a smaller repulsion energy. Remarkably, the two trinitrotoluene isomers attain exactly the same lattice energy, although with a different combination of the various contributions. The 2,3,4-isomer has a higher lattice density which in this case favors higher dispersion energy contributions, but the 3,4,5-isomer compensates with a higher Coulombic contribution.

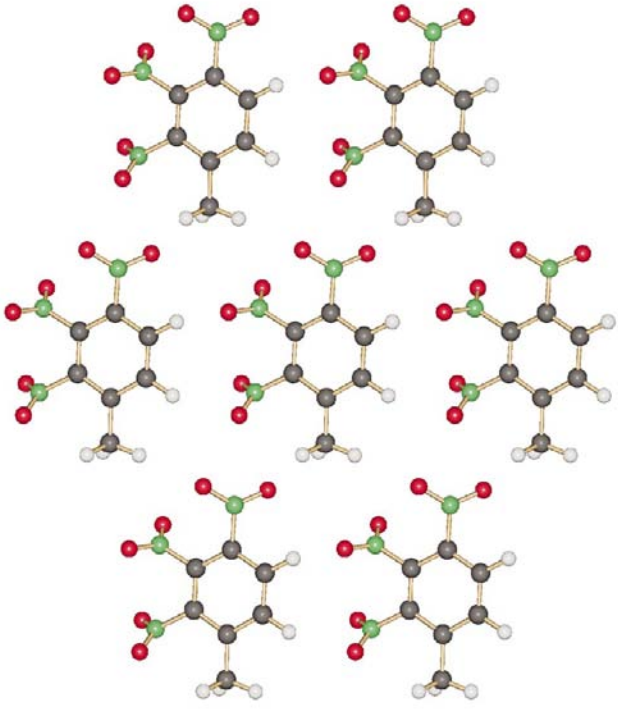

Figure 12
Layering by pure translation in the crystal structure of K20 (*ac* plane, origin is at the top left).

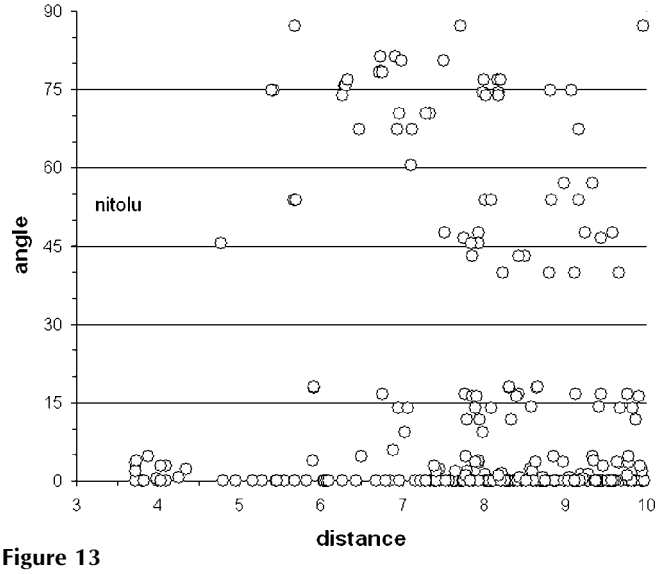

Figure 13
A scatterplot of angles between benzene ring planes (°) and distance between benzene ring centroids (Å) over all the crystal structures considered. The outlier is in the crystal structure of nitrotoluene and its structure shown in Fig. 14.

Table 8
Lattice-dynamical calculated crystal properties.

Energies in kJ mol^{-1}, entropies in J K^{-1} mol^{-1} (standard: 1 atm), lattice vibration frequencies in cm^{-1}, vapor pressure in mPa.

Crystal	External S	ΔS(subl)	ν range	Substituent type	UNI lattice energy	Vapor pressure
K6	113	200	26–150	Intermolecular hydrogen bond	139	10^{-6}
K12 = MNIAAN10	122	184	26–176	Intermolecular hydrogen bond	119	0.0014
MNIAAN01	116	191	20–88	Intramolecular hydrogen bond	118	0.010
K19	127	183	17–103	NO_2, CH_3	112	0.012
K20	123	187	21–118	NO_2, CH_3	120	0.0030
BAFLEZ	126	183	33–104	Cl, NO_2, CH_3	108	0.33
DNBENZ10	126	178	11–94	NO_2	101	1.3
ZZZFYW01	123	171	30–93	NO_2	101	0.8
NITOLU	128	164	13–109	NO_2, CH_3	86	130
TNBENZ10	119	191	12–116	NO_2	105	2.1
ZZZGVU01	122	182	20–113	NO_2, CH_3	109	0.11
ZZZQSC	113	190	19–106	NO_2, CH_3	108	0.51
ZZZMUC01	113	200	15–114	NO_2, CH_3	119	0.023
ZZZMUC06	113	200	21–114	NO_2, CH_3	119	0.022

The calculated lattice energies compare reasonably well with the few heats of sublimation available. The Pixel calculation does not reproduce the differences in heats of sublimation among the three dinitrobenzene isomers, with the substantially higher stability of the 1,4-dinitrobenzene isomer crystal. This effect is instead inferred by the less accurate, but more heavily parameterized UNI force-field.

6. Lattice dynamics

Table 8 collects the calculated external entropies, entropies of sublimation, lattice vibrational frequencies (at the origin of the Brillouin zone) and estimated vapor pressures for some selected compounds. The method and assumptions for their derivation have been described and examined (Gavezzotti & Filippini, 1997). Essentially, the procedure rests on the main assumption of invariance of internal vibrations between gas phase and crystal, as well as on the non-mixing of internal and external vibrational modes. Besides, there is an obvious dependence of the quality of the results on the quality of the potentials. In a few cases, among those appearing in Tables 1 and 2, but not in Table 8, the lattice-dynamical calculation did not converge properly (imaginary frequencies or other computational troubles). Fig. 16 shows the *ORTEP*II plot (Johnson, 1976) for the six molecules whose crystal structures have been determined in this work. Remarkably enough, irrespective of molecular composition, the lattice-vibrational entropy varies in a very narrow range, 113–128 J K^{-1} mol^{-1}, and, correspondingly, so does the entropy of sublimation. In particular, external entropy differences between crystal structures of isomers or between polymorph crystal structures are negligible, as already noted when assessing the relative importance of entropic effects in attempted crystal structure predictions (Boese *et al.*, 2001). The upper limit of the lattice-vibrational frequencies is higher in the intermolecularly hydrogen-bonded crystals, but is in the 15–120 cm^{-1} range for all other compounds considered. The estimated crystal vapor pressures follow the trend of sublimation enthalpies, given the relative invariance of the sublimation entropies.

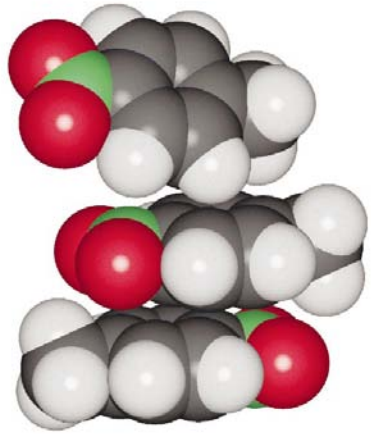

Figure 14
Close neighbors in the crystal structure of nitrotoluene: A, I determinant in Table 6 (symmetry code: $-x, -y, -z$); B, G determinant in Table 6, with an unusually short ring–ring distance for a high ring–ring angle (symmetry code: $\frac{1}{2}+x, \frac{1}{2}-y, z$). Short C$\cdots$H distances are 3.3–3.4 Å.

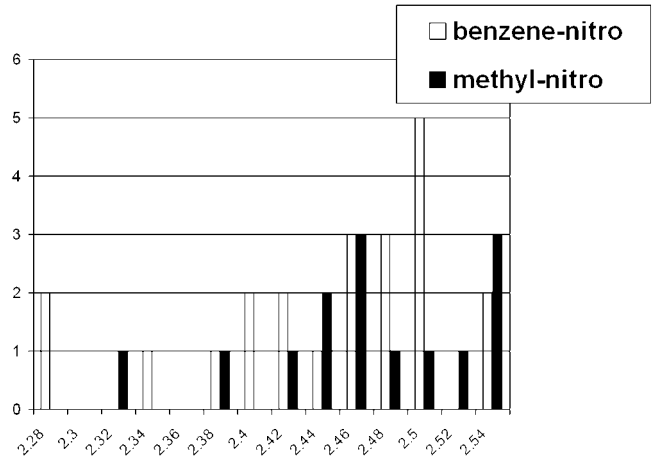

Figure 15
Frequency of H$\cdots$O(nitro) atom–atom distances. Bins are given in Å.

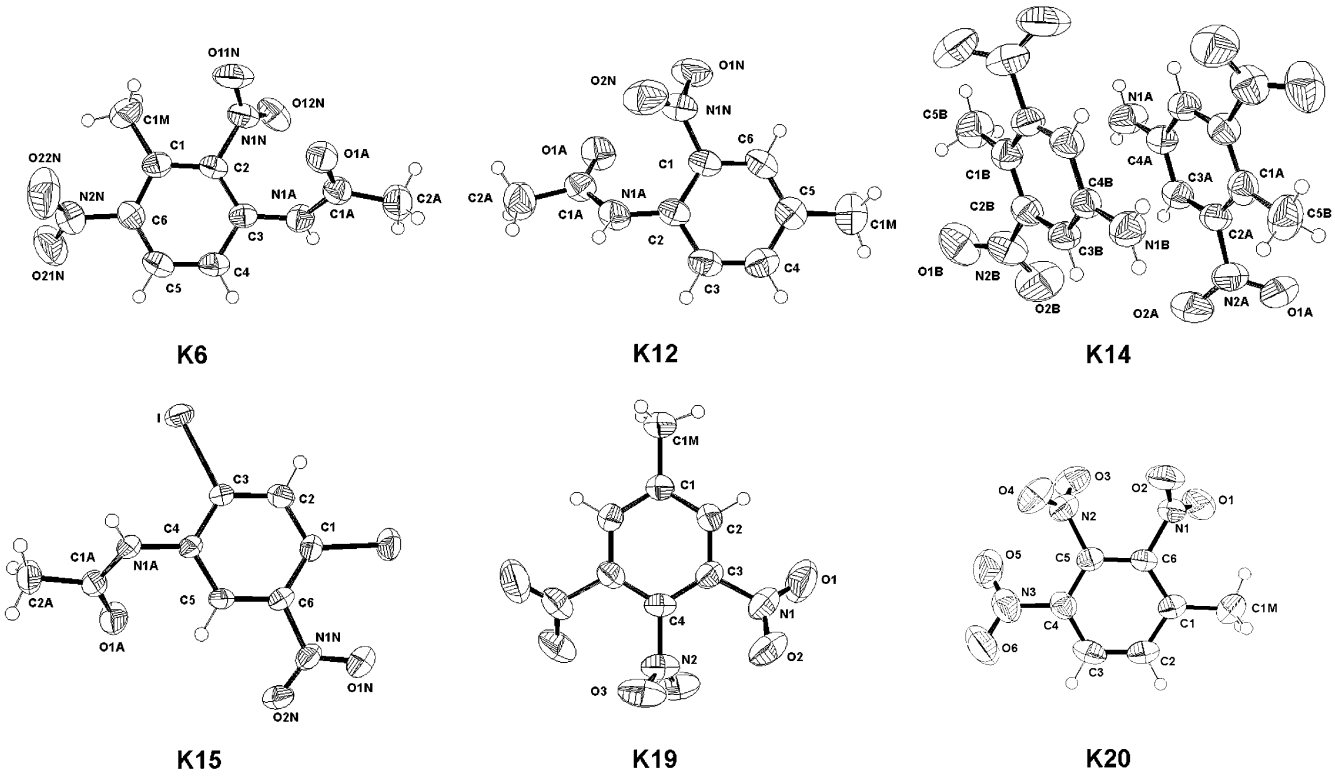

Figure 16
*ORTEP*II (Johnson, 1976) plots drawn at 50% probability.

The *OPiX* computer program package is available for distribution for a nominal fee. Requests should be addressed to angelo.gavezzotti@unimi.it.

We thank Professor Lucio Merlini, Director of the Dipartimento di Scienze Molecolari Agroalimentari of the University of Milano, for permission to visit the Koerner site and for generously donating the samples, and Professor Anna Arnoldi for help in the retrieval of the crystal samples. Figures were drawn with the help of the program *SCHAKAL*.

References

Allen, F. H. (2002). *Acta Cryst.* B**58**, 380–388.
Artini, E. (1905). *Rend. Ist. Lomb. Acad. Sci. Lett. Ser. II*, **XXXVIII**, 831–853.
Artini, E. (1918). *Rend. Ist. Lomb. Acad. Sci. Lett. Ser. II*, **LI**, 961–989.
Boese, R., Kirchner, M. T., Dunitz, J. D., Filippini, G. & Gavezzotti, A. (2001). *Helv. Chim. Acta*, **84**, 1561–1577.
Burla, M. C., Camalli, M., Carrozzini, B., Cascarano, G., Giacovazzo, C., Polidori, G. & Spagna, R. (2001). *J. Appl. Cryst.* **34**, 523–526.
Day, G. M. & Motherwell, W. D. S. (2003). Personal communication.
Farrugia, L. J. (1999). *J. Appl. Cryst.* **32**, 837–838.
Filippini, G. & Gavezzotti, A. (1994). *Chem. Phys. Lett.* **231**, 86–92.
Frisch, M. J. *et al.* (1998). *Gaussian*98, Revision A.7. Gaussian, Inc., Pittsburgh, PA, USA.
Gavezzotti, A. (2002). *J. Phys. Chem. B*, **106**, 4145–4154.
Gavezzotti, A. (2003*a*). *OPiX*. University of Milano, Italy.
Gavezzotti, A. (2003*b*). *J. Phys. Chem. B*, **107**, 2344–2356.
Gavezzotti, A. (2003*c*). *Cryst. Eng. Commun.* **5**, 429–438.
Gavezzotti, A. (2003*d*). *Cryst. Eng. Commun.* **5**, 439–446.
Gavezzotti, A. & Filippini, G. (1994). *J. Phys. Chem.* **98**, 4831–4837.
Gavezzotti, A. & Filippini, G. (1995). *J. Am. Chem. Soc.* **117**, 12299–12305.
Gavezzotti, A. & Filippini, G. (1997). *Theoretical Aspects and Computer Modeling of the Molecular Solid State*, edited by A. Gavezzotti. Chichester: Wiley and Sons.
Gramaccioli, C. M. & Filippini, G. (1984). *Chem. Phys. Lett.* **108**, 585–588.
Johnson, C. K. (1976). *ORTEP*II. Report ORNL 5138. Oak Ridge National Laboratory, Tennessee, USA.
Keller, E. (1999). *SCHAKAL*99. University of Freiburg, Germany.
Lommerse, J. P. M., Stone, A. J., Taylor, R. & Allen, F. H. (1996). *J. Am. Chem. Soc.* **118**, 3108–3116.
McBride, M. (1980). *J. Am. Chem. Soc.* **102**, 4134–4137.
Moore, J. C., Yeadon, A. & Palmer, R. A. (1983). *J. Crystallogr. Spectrosc. Res.* **13**, 279–286.
Rowland, R. S. & Taylor, R. (1996). *J. Phys. Chem.* **100**, 7384–7391.
Sheldrick, G. M. (1996). *SADABS*. University of Göttingen, Germany.
Sheldrick, G. M. (1997). *SHELX*97. University of Göttingen, Germany.
Watkin, D. (2003). Personal communication.